Journal of Engineering Mathematics, Vol. 14, No. 2, April 1980

On the relation between adjacent inviscid cell type solutions to the rotating-disk equations.

D. DIJKSTRA

Department of Applied Mathematics, Twente University of Technology, Enschede, The Netherlands

(Received October 25, 1979)

SUMMARY

Over a large range of the axial coordinate a typical higher-branch solution of the rotating-disk equations consists of a chain of inviscid cells separated from each other by viscous interlayers. In this paper the leading-order relation between two adjacent cells will be established by matched asymptotic expansions for general values of the parameter appearing in the equations. It is found that the relation between the solutions in the two cells crucially depends on the behaviour of the tangential velocity in the viscous interlayer. The results of the theory are compared with accurate numerical solutions and good agreement is obtained.

1. Introduction

During the past decade a number of interesting properties of solutions to the similarity rotating-disk equations have been established. At present it is known that the solution to the similarity equations for a single disk is non-unique. In fact, Zandbergen en Dijkstra [8] showed by means of adequate numerical techniques that branching of the solution occurs at certain values of the parameter s. Here s denotes the ratio of the tangential velocities of the fluid at infinity and at the disk. According to further investigations [9] there are infinitely many solutions to the problem in a small region near $s = 0$. When two neighbouring branches are compared it is found that the main difference between the solutions consists of an extra inviscid cell which is built up as the solution proceeds from one branch into the other. Near the disk as well as near infinity the solutions are almost indistinguishable from each other in particular when higher branches are compared.

Over a large range of the axial coordinate a typical higher-branch solution consists of a chain of inviscid cells separated from each other by viscous interlayers. The solution ends with viscous regions both near the disk and near infinity. In order to get more insight in the structure of a chain of inviscid cells the present investigation was performed.

Solutions of inviscid cell type have been considered earlier in papers by Kuiken [5], Ockendon [7] and Bodonyi [2]. Kuiken and Bodonyi use one cell only in their work while Ockendon indicated the possibility of a chain of inviscid cells but she did not work out the details of the argument necessary to match one cell with another. To leading order this match of two inviscid cell type solutions will be performed in the present paper and it appears that the behaviour of the tangential velocity in the viscous interlayer is crucial to the nature of the relation between the solutions in the two cells.

The paper by Kuiken [5] has been taken as a starting point for the present work and his

expansion, valid for $s = 0$, will be generalized to arbitrary values of s. The relation between two adjacent inviscid cell type solutions will be given in the form of a theorem contained in Sec. 4 and in the sequel an inviscid cell type solution will be called 'large hill' because of the shape of the axial velocity in such a cell.

2. Preliminary analysis

In this section a preliminary consideration is made to obtain an inviscid solution to the equations. The result will be used in Sec. 3 as a starting point for the expansion of the solution. Let f, $-f'$, g respectively denote the non-dimensional axial, radial and tangential velocities and let x be the non-dimensional axial coordinate. Consider the set of differential equations for the rotating disk.

$$\begin{aligned} &f''' - ff'' + \tfrac{1}{2}f'^2 - 2g^2 = -2s^2, \\ &g'' - fg' + f'g = 0. \end{aligned} \qquad \left(' = \frac{d}{dx}\right) \tag{2.1}$$

Here, the function f differs by a factor -2 from the one used elsewhere. Suppose that in some region the highest derivatives may be neglected which means that the solution is inviscid in such a region. The system (2.1) then becomes

$$\begin{aligned} &-ff'' + \tfrac{1}{2}f'^2 - 2g^2 = -2s^2, \\ &-fg' + f'g = 0, \end{aligned} \qquad f'(0) = 0, \tag{2.2}$$

where the origin $x = 0$ has been located via the boundary condition on f'. The system (2.2) can be solved exactly and the solution which satisfies the boundary condition is

$$\pm g = \mu f \quad , \quad f = \lambda \cos^2(\mu x) + C \quad , \quad \mu \geqslant 0 \tag{2.3}$$

where

$$2C = -\lambda \pm \sqrt{\lambda^2 + 4s^2/\mu^2} \tag{2.4}$$

while λ and μ are arbitrary constants. The non-negativity of μ does not imply a loss of generality.

From numerical solutions relevant to large inviscid regions (Zandbergen, Dijkstra [4, 9]) it emerges that λ is large and positive while $|C| \ll \lambda$. Hence, we choose the upper sign in (2.4) so that

$$2C = -\lambda + \sqrt{\lambda^2 + 4s^2/\mu^2} = \frac{4s^2/\mu^2}{\lambda + \sqrt{\lambda^2 + 4s^2/\mu^2}} \cdot \tag{2.5}$$

Note that the constant C vanishes at $s = 0$ and (2.3) coincides with the result found by Kuiken [5] in that case. The present theory is valid for general values of s and therefore constitutes a generalization of the Kuiken theory.

On the basis of (2.3) the individual terms appearing in (2.1) can now be estimated in terms of λ and μ as follows

$$f''' \ , \ g'' = O(\lambda\mu^3) \ , \ s^2 = O(1),$$

$$ff'' \ , \ f'^2 \ , \ g^2 \ , \ fg' \ , \ f'g = O(\lambda^2\mu^2),$$

so that the condition

$$\lambda\mu^3 \ll \lambda^2\mu^2 \Leftrightarrow \mu/\lambda \ll 1 \tag{2.6}$$

justifies the negligibility of the highest derivatives f''' and g''. For extended inviscid regions encountered by Zandbergen and Dijkstra [4, 9] condition (2.6) was found to be satisfied. In particular they observed

$$f = O(\lambda) \gg 1 \quad , \quad |g|/f = O(\mu) \ll 1 \quad , \quad f'' = O(\lambda\mu^2) = O(1) \tag{2.7}$$

which may be written in the form of the following limit

$$\lambda \to \infty \quad , \quad \mu \to 0^+ \quad , \quad \lambda\mu^2 \to A > 0. \tag{2.8}$$

Note that in this limit the conditions (2.7) and hence (2.6) are satisfied. Although (2.6) is satisfied under less severe conditions on λ and μ we shall restrict ourselves to the limit (2.8) in view of (2.7).

Since we will only consider leading-order effects, the constant C given by (2.5) may be replaced by its asymptotic value (for convenience later on), viz.

$$\tilde{C} = s^2/(\lambda\mu^2). \tag{2.9}$$

In the limit (2.8) this is a finite number and the error $|C - \tilde{C}|$ is of order $1/\lambda$. With C in (2.3) replaced by $\tilde{C}$ we may state that

$$f(x) = \lambda\cos^2(\mu x) + \tilde{C} \quad , \quad \pm g = \mu f \quad , \quad \tilde{C} = s^2/(\lambda\mu^2) \tag{2.10}$$

is an inviscid approximation to certain solutions of (2.1) in the limit (2.8).

Solutions of the form (2.10) will be called 'large hills' because of the shape of the function f, which is large while g is much smaller. The range over which the hill extends constitutes one 'cell' given by

$$-\frac{\pi}{2\mu} \leqslant x \leqslant +\frac{\pi}{2\mu} \tag{2.11}$$

and the longer this range is, the better the approximation (2.10) appears to be.

The parameters λ and μ will now be defined in such a way that (2.10) coincides with $f(0)$ and $g(0)$ at the origin. To achieve this we must set

$$f(0) = \lambda + \tilde{C} \quad , \quad \pm g(0) = \mu f(0),$$

or explicitly

$$\mu = \pm g(0)/f(0) \quad , \quad \lambda = \tfrac{1}{2} f(0) \{1 + \sqrt{1 - (2s/g(0))^2}\}. \tag{2.12}$$

The limit (2.8) is now recovered if

$$f(0) \gg 1 \quad , \quad g^2(0) \sim A f(0) \quad , \quad A > 0. \tag{2.13}$$

3. Expansion procedure for large hills

On the basis of the considerations in Sec. 2 we will set up an expansion to approximate large-hill solutions and three terms will be calculated.

Suppose that over a certain range of the coordinate x a solution to eqs. (2.1) is of large-hill type as defined in Sec. 2. With origin at the top of the hill ($f'(0) = 0$) it is assumed that (2.13) holds. The parameters λ and μ are defined by means of (2.12) with $\pm$ = sign ($g(0)$). At the origin we then have

$$f'(0) = 0 \quad , \quad f(0) = \lambda + \tilde{C} \quad , \quad g(0) = \pm \mu(\lambda + \tilde{C}) \tag{3.1}$$

where $\tilde{C}$ is given by (2.9).

As a consequence of (2.13) the limit (2.8) applies and it follows that $\mu = O(\lambda^{-\frac{1}{2}})$. In principle, the expansion could be set up in terms of one parameter, but if both λ and μ are used the structure becomes more clear.

We now rescale the variables in such a way that the large-hill solution (2.10) as well as the cell range (2.11) remain of order $O(1)$ in the limit (2.8):

$$f(x) = \lambda F(\xi) \quad , \quad g(x) = \pm \lambda\mu G(\xi) \quad , \quad \xi = \mu x. \tag{3.2}$$

In terms of the new variables the equations (2.1) and (3.1) become

$$FF'' - \tfrac{1}{2} F'^2 + 2G^2 = 2\tilde{C}/\lambda + \mu F'''/\lambda \quad , \quad \tilde{C} = s^2/(\lambda\mu^2) = O(1),$$

$$FG' - F'G = \mu G''/\lambda, \qquad (' = d/d\xi) \tag{3.3}$$

$$F'(0) = 0 \quad , \quad F(0) = G(0) = 1 + \tilde{C}/\lambda.$$

The inviscid nature of the differential equations now follows from the smallness of μ/λ in the right-hand sides, which suggest the following expansion in the limit (2.8)

$$F(\xi) = F_0(\xi) + \frac{1}{\lambda} F_1(\xi) + \frac{\mu}{\lambda} F_2(\xi) + O\left(\frac{1}{\lambda^2}\right),$$
$$G(\xi) = G_0(\xi) + \frac{1}{\lambda} G_1(\xi) + \frac{\mu}{\lambda} G_2(\xi) + O\left(\frac{1}{\lambda^2}\right). \tag{3.4}$$

Substitution of these expansions into (3.3) produces a hierarchy of problems for the functions F_i and G_i similar to the structure derived by Kuiken [5]:

$$\begin{aligned} &F_0F_0'' - \tfrac{1}{2}F_0'^2 + 2G_0^2 = 0 \quad , \quad F_0(0) = 1 \quad , \quad F_0'(0) = 0, \\ &F_0G_0' - F_0'G_0 \qquad = 0 \quad , \quad G_0(0) = 1; \end{aligned}$$

$$\begin{aligned} &F_0F_1'' + F_0''F_1 - F_0'F_1' + 4G_0G_1 = 2\mathcal{C} \quad , \quad F_1(0) = \mathcal{C} \quad , \quad F_1'(0) = 0, \\ &F_0G_1' + F_1G_0' - F_0'G_1 - F_1'G_0 \quad = 0 \quad , \quad G_1(0) = \mathcal{C}; \end{aligned}$$

$$\begin{aligned} &F_0F_2'' + F_0''F_2 - F_0'F_2' + 4G_0G_2 = F_0''' \quad , \quad F_2(0) = F_2'(0) = 0, \\ &F_0G_2' + F_2G_0' - F_0'G_2 - F_2'G_0 \quad = G_0'' \quad , \quad G_2(0) = 0. \end{aligned}$$

These problems can be exactly solved (Dijkstra [4A], Kuiken [5]) and (3.4) becomes

$$F(\xi) = \cos^2\xi + \frac{\mathcal{C}}{\lambda} + \frac{\mu}{\lambda}\left\{-\tfrac{8}{3}\sin 2\xi \ln(\cos\xi)\right\} + O\left(\frac{1}{\lambda^2}\right),$$
$$G(\xi) = F(\xi) + \frac{\mu}{\lambda}\left\{\tfrac{2}{3}\tan\xi - \tfrac{4}{3}\sin 2\xi\right\} + O\left(\frac{1}{\lambda^2}\right). \tag{3.5}$$

The simplicity of the second term F_1/λ is a consequence of the special definition of the parameters λ and μ. In addition the second term represents the main effect of the parameter s in the equations (2.1). At $s = 0$ the constant $\mathcal{C}$ vanishes and in this case the result (3.5) is found to coincide with the result derived by Kuiken [5]. Therefore the present theory is a generalization of the Kuiken expansion.

Differentiation of (3.5) yields in terms of the original variables at the origin $x = 0$:

$$f''(0) = -2\lambda\mu^2 + O(1/\lambda^2) \quad , \quad g'(0) = \mp 2\mu^3 + O(1/\lambda^2). \tag{3.6}$$

In the limit (2.8) we also have

$$\lambda\mu^2 \to A \sim -f''(0)/2. \tag{3.7}$$

Indeed, these relations are found to be valid for the large-hill solutions encountered in [4, 9], which checks the consistency of the theory above.

Clearly, the approximation (3.5) to the phenomenon which we call a large hill is accurate

over most part of the range $|\xi| \leqslant \pi/2$, but it fails near the end points of the cell. We first consider the left end and set

$$\xi = -\pi/2 + \xi_1 \quad , \quad \xi_1 \downarrow 0. \tag{3.8}$$

Expanding (3.5) for $\xi_1 \to 0^+$ we find

$$F(\xi) \sim (\xi_1^2 - \tfrac{1}{3}\xi_1^4 + \ldots) + \frac{\tilde{C}}{\lambda} + \frac{\mu}{\lambda}\{\tfrac{16}{3}\xi_1 \ln \xi_1 + O(\xi_1^3 \ln \xi_1)\},$$

$$G(\xi) \sim F(\xi) + \frac{\mu}{\lambda}\{-\tfrac{2}{3}\frac{1}{\xi_1} + \tfrac{26}{9}\xi_1 + O(\xi_1^3)\}. \tag{3.9}$$

The leading term ξ_1^2 is seen to be of the same order as the second term $\tilde{C}/\lambda$ if $\xi_1 = O(\lambda^{-1/2}) = O(\mu)$. For values of ξ_1 of that order we rearrange (3.9) and multiply by λ whence

$$\lambda F(\xi) \sim (\lambda\xi_1^2 + \tilde{C}) + \mu(\tfrac{16}{3}\xi_1 \ln \xi_1) - \tfrac{1}{3}\lambda\xi_1^4 + \ldots,$$

$$\lambda G(\xi) \sim (\lambda\xi_1^2 + \tilde{C} - \tfrac{2}{3}\frac{\mu}{\xi_1} + \ldots) + \mu(\tfrac{16}{3}\xi_1 \ln \xi_1) + \tag{3.10}$$

$$+ (\tfrac{26}{9}\mu\xi_1 - \tfrac{1}{3}\lambda\xi_1^4 + \ldots).$$

Inspection of (3.10) shows that if $\xi_1 = O(\mu) = O(\lambda^{-1/2})$ the first term is $O(1)$, the second one is $O(\mu^2 \ln \mu)$ and the third term is $O(\mu^2)$. Hence, a new hierarchy of terms has been constructed with λF and λG of order $O(1)$ provided that $\xi_1/\mu = O(1)$. From (3.2) and (3.8) it then follows that appropriate inner variables are

$$f(x_1) \quad , \quad g(x_1)/\mu \quad , \quad x_1 = x + \pi/(2\mu) = \xi_1/\mu. \tag{3.11}$$

These variables should be used for the description of the solution in a comparatively small region near $x_1 = 0$ and a matching argument ($\xi_1 \to 0, x_1 \to \infty$) applied to (3.10) yields the following asymptotic behaviour for the quantities (3.11):

$$f(x_1) = (\lambda\mu^2 x_1^2 + \tilde{C}) + O(\mu^2 \ln \mu),$$

$$\pm \frac{g(x_1)}{\mu} = \left(\lambda\mu^2 x_1^2 + \tilde{C} - \frac{2}{3x_1} + \ldots\right) + O(\mu^2 \ln \mu). \qquad (x_1 \to \infty) \tag{3.12}$$

In Fig. 3.1. a large hill has been depicted and an attempt has been made to visualize the matching argument given above.

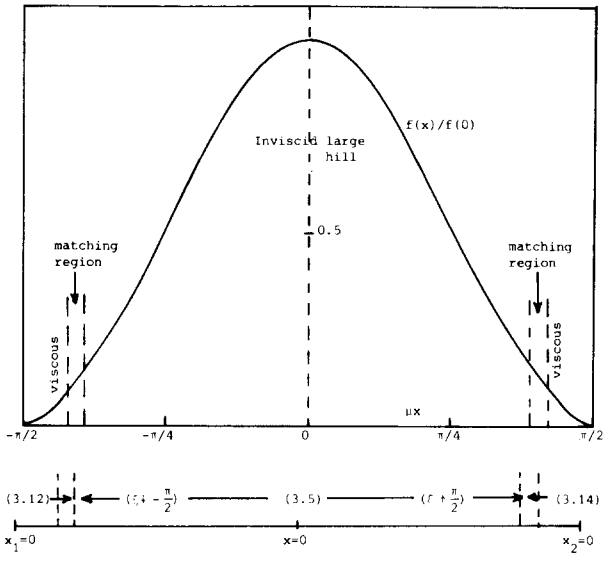

Figure 3.1 Large-hill solution matching at its feet with viscous solutions.

The other foot of the hill ($\xi = \mu x = +\pi/2$) can be investigated in the same way and the relevant inner variables are

$$f(x_2) \quad , \quad g(x_2)/\mu \quad , \quad x_2 = x - \pi/(2\mu) \tag{3.13}$$

with asymptotic behaviour

$$f(x_2) = (\lambda\mu^2 x_2^2 + \tilde{C}) + O(\mu^2 \ln \mu),$$

$$\pm \frac{g(x_2)}{\mu} = \left(\lambda\mu^2 x_2^2 + \tilde{C} - \frac{2}{3x_2} + \ldots \right) + O(\mu^2 \ln \mu). \qquad (x_2 \to -\infty) \tag{3.14}$$

Since exponentially small solutions may be added on to (3.14) the continuation of the solution outside the cell for $x_2 \to +\infty$ is non-unique. According to Ockendon [7] there are at least two possible continuations (I and II):

Case I. This is the case where

$$f' \to 0 \quad , \quad g \to s \quad , \quad x_2 \to +\infty$$

with exponentially small error. This possibility was investigated by Kuiken [5] for the case $s = 0$.

Case II. The other possible solution becomes inviscid again beyond $x_2 = 0$, in other words a second cell exists for $x_2 > 0$ and the solution considered above merges into the new cell via a

viscous interlayer centered at $x_2 = 0$. For general values of s, this possibility will be investigated in the next section.

4. The viscous interlayer between two large hills

In this section we will consider two adjacent large hills with parameters $(\lambda_i,\mu_i)(i = 1,2)$. The two hills (Fig. 4.1) are separated from each other by a viscous interlayer and it will appear that the behaviour of the tangential velocity g in this layer is of crucial importance to the relation between the two large-hill solutions.

It will be assumed that the limit (2.8) applies to both hills, viz.

$$\lambda_i \to \infty \quad , \quad \mu_i \to 0^+ \quad , \quad \lambda_i \mu_i^2 \to A_i > 0 \quad (i = 1,2) \tag{4.1}$$

where λ_i and μ_i are defined by (2.12) with $f(0)$ and $g(0)$ replaced by the values at P_i $(i = 1,2$; Fig. 4.1). In the limit (4.1) the results of Sec. 3 are valid for both hills and suitable $O(1)$ variables in the viscous interlayer are given by (3.11) or (3.13) with μ replaced by μ_1 or μ_2 respectively. Of these we will choose (3.11) so that the reference scale of g in the viscous interlayer will be μ_1. The appropriate independent variable is the unscaled x-coordinate of which the present origin is located at P_0 (Fig. 4.1) where $f' = 0$. Since the origins of the coordinates x_i given by (3.11) and (3.13) do not necessarily coincide with P_0 we set

$$x_1 = x + \Delta_1 \quad , \quad x_2 = x + \Delta_2 \tag{4.2}$$

and it will appear that the shifts Δ_i vanish to *leading* order.

The expansion of the solution in the viscous interlayer, suggested by (3.12) is now taken as

$$\begin{aligned} f(x) &= f_0(x) + \mu_1^2 \ln\mu_1 \, f_1(x) + \ldots , \\ g(x) &= \pm \mu_1 \{ g_0(x) + \mu_1^2 \ln\mu_1 \, g_1(x) + \ldots \}, \end{aligned} \tag{4.3}$$

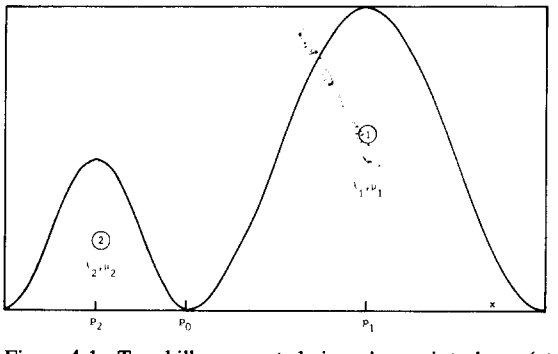

Figure 4.1 Two hills connected via a viscous interlayer (at points P_i: $f' = 0$).

where $\pm$ = sign $g(P_1)$. We restrict ourselves to a consideration of the leading order governed by the equations

$$\begin{aligned} &f_0''' - f_0 f_0'' + \tfrac{1}{2} f_0'^2 = -2s^2, \\ &g_0'' - f_0 g_0' + f_0' g_0 = 0. \end{aligned} \qquad (' = d/dx \quad , \quad f_0'(0) = 0) \tag{4.4}$$

These equations are obtained if (4.3) is substituted into (2.1) and the asymptotic boundary conditions are found from (3.12) with (λ,μ) replaced by (λ_1,μ_1) and from (3.14) with (λ,μ) replaced by (λ_2,μ_2):

$$\begin{aligned} &f_0(x) \sim \lambda_1 \mu_1^2 (x+\Delta_1)^2 + \mathcal{C}_1 \quad , \quad x \to +\infty, \\ &f_0(x) \sim \lambda_2 \mu_2^2 (x+\Delta_2)^2 + \mathcal{C}_2 \quad , \quad x \to -\infty, \\ &g_0(x) \sim \lambda_1 \mu_1^2 (x+\Delta_1)^2 + \mathcal{C}_1 - \frac{2}{3(x+\Delta_1)} + \dots \quad , \quad x \to +\infty, \\ &g_0(x) \sim \frac{\pm\mu_2}{\pm\mu_1} \left\{ \lambda_2 \mu_2^2 (x+\Delta_2)^2 + \mathcal{C}_2 - \frac{2}{3(x+\Delta_2)} + \dots \right\} , \quad x \to -\infty, \end{aligned} \tag{4.5}$$

where x_i has been replaced by $(x+\Delta_i)$, eq. (4.2), and the constants $\mathcal{C}_i$ are

$$\mathcal{C}_i = s^2/(\lambda_i \mu_i^2). \tag{4.6}$$

The asymptotic condition for $x \to +\infty$ uniquely determines the function f_0. From the Appendix we infer

$$f_0(x) \equiv \lambda_1 \mu_1^2 (x+\Delta_1)^2 + \mathcal{C}_1, \tag{4.7}$$

and since $f_0'(0) = 0$ the shift Δ_1 must vanish (to the order considered). The condition (4.5) on f_0 as $x \to -\infty$ now yields

$$\mathcal{C}_1 = \mathcal{C}_2 \quad ; \quad \Delta_1 = \Delta_2 = 0 \quad ; \quad \lambda_1 \mu_1^2 = \lambda_2 \mu_2^2 \tag{4.8}$$

all valid to the order considered. Hence the limits A_i (4.1) must be the same:

$$A_1 = A_2 = A \text{ (say)} \tag{4.9}$$

and (4.7) becomes

$$f_0(x) = Ax^2 + s^2/A \quad , \quad A = \lambda_1 \mu_1^2 = \lambda_2 \mu_2^2, \tag{4.10}$$

In other words the quantity $f''(x)$ approaches the same limit as one leaves the viscous interlayer in either direction provided that (4.1) can be applied.

With the simple result (4.10) for f_0 we now consider the problem for g_0. On the basis of eqs (4.4) – (4.10) together with the definitions

$$t = xA^{1/3} \quad , \quad \bar{g}(t) = A^{-1/3} g_0(x),$$
$$a = s^2/A^{4/3} \quad , \quad \rho = \pm\mu_2/\pm\mu_1 , \tag{4.11}$$

the standardized problem governing the function g in the viscous interlayer can be written as

$$\bar{g}'' - (t^2 + a)\bar{g}' + 2t\bar{g} = 0, \qquad (' = d/dt)$$
$$\bar{g} \sim t^2 + a - \frac{2}{3t} + \ldots , \qquad t \to +\infty, \tag{4.12}$$
$$\bar{g} \sim \rho \left(t^2 + a - \frac{2}{3t} + \ldots \right), \qquad t \to -\infty.$$

As in the case of f_0 the asymptotic condition with $t \to +\infty$ uniquely determines the solution $\bar{g}$ for each value of the parameter $a \geq 0$ and this solution determines the value of ρ in the asymptotic behaviour for $t \to -\infty$. Hence the problem (4.12) implicitly defines a function $\rho(a)$ from which the ratio of the μ_i then follows with (4.11). At both ends $t = \pm\infty$ the second derivatives $\bar{g}''$ are finite and they will differ in value depending on the parameter a. To leading order the function $g''(x)$ will therefore tend to different limits as $x \to \pm\infty$ and the ratio of these limits is equal to $\rho(a)$. The results given above can now be summarized in the form of the following theorem (for relevant configuration see Fig. 4.1):

Theorem (leading-order match). Let

$$\lambda_1\mu_1^2 = A > 0 \quad , \quad a = s^2/A^{4/3}$$

and let $\rho(a)$ be defined by (4.12). Then to leading order in the limit (4.1)

$$\lambda_1\mu_1^2 = \lambda_2\mu_2^2 = A_1 = A_2 = A \quad ; \quad \mu_2/\mu_1 = |\rho| \quad , \quad \lambda_1/\lambda_2 = \rho^2 . \tag{4.13}$$

Furthermore

$$\operatorname{sign} g(P_1)/\operatorname{sign} g(P_2) = \operatorname{sign} \rho(a).$$

In case $\rho(a) = 0$, the leading-order approximation to the function $g(x)$ becomes exponentially small to the left of P_0 (Fig. 4.1) while the leading-order term for $f(x)$ is the parabola (4.10) which continues indefinitely as $x \to -\infty$. (For this and other special cases see Sec. 5)

The fundamental function $\rho(a)$ defined by (4.12) determines the leading-order relation between two adjacent large hills via (4.13). For $a \in [0,\infty]$ the function $\rho(a)$ has been calculated numerically and this will be considered in the next section.

5. Properties of the fundamental function ρ

5.1 Numerical calculation of $\rho(a)$

For a given value of $a \geqslant 0$ the quantity $\rho(a)$ can be computed from its definition (4.12). The differential equation (4.12) for $\bar{g}$ has been integrated numerically with the Bulirsch and Stoer method [3], starting at $t = T$ with asymptotic values for $\bar{g}(T)$ and $\bar{g}'(T)$ and integrating down to $t = -T$. From the results obtained at $t = -T$ the factor ρ in (4.12) can then be calculated. Use has been made of an asymptotic expansion of the solution $\bar{g}$ with error $O(t^{-8})$ and it appeared that $T = 9$ is large enough to determine $\rho(a)$ in at least 8 places of decimals. For the details, see Dijkstra [4A]. The results $\rho(a)$ have been tabulated in Table 5.1 and graphically represented in Fig. 5.1. It is clear that ρ monotonically increases from -2 to 1 as a increases from 0 to ∞. The solution $\bar{g}(t)$ of the problem (4.12) and its second derivative have been depicted in Figs. 5.2 and 5.3 and it will be clear that the approximation $t^2 + a$ $(t \to \infty)$ smoothly changes into $\rho(a)$ $(t^2 + a)$ $(t \to -\infty)$ over a restricted range of the argument t. For further details, see Dijkstra [4A].

TABLE 5.1

The function ρ and its asymptotic approximation ρ_{as} (a).

a	ρ (a)	ρ_{as} (a) (6.7)	error $* 10^7$
0	− 2	− 1	
0.02	− 1.94095034	− 0.997	
0.05	− 1.85539448	− 0.988	
0.10	− 1.72041018	− 0.968	
0.20	− 1.47627152	− 0.911	
0.30	− 1.26218996	− 0.841	
0.40	− 1.07370223	− 0.765	
0.50	− 0.90709938	− 0.684	
0.60	− 0.75928628	− 0.601	
0.70	− 0.62766944	− 0.517	
0.80	− 0.51006697	− 0.434	
0.90	− 0.40463603	− 0.354	
1.00	− 0.30981423	− 0.276	
1.25	− 0.11091888	− 0.099	
1.50	+ 0.04552998	+ 0.04966862	+ 41386
2.00	+ 0.27201985	+ 0.27252637	+ 5065
2.50	+ 0.42466748	+ 0.42472665	+ 592
3.00	+ 0.53232449	+ 0.53232688	+ 24
4.00	+ 0.67061434	+ 0.67061198	− 24
5.00	+ 0.75315918	+ 0.75315840	− 8

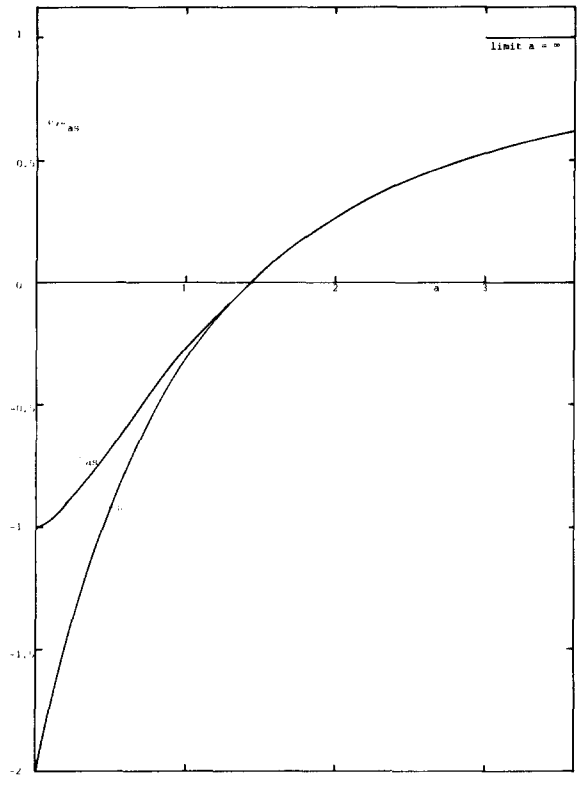

Figure 5.1 The functions $\rho(a)$ and $\rho_{as}(a)$.

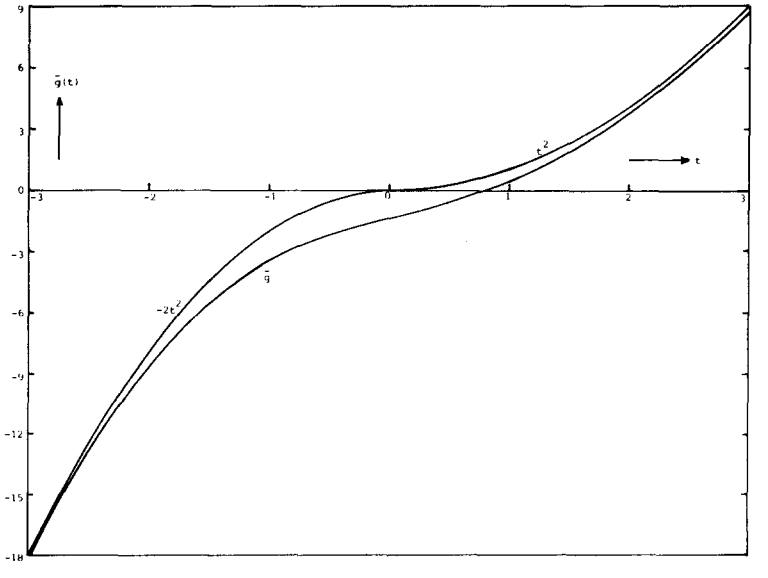

Figure 5.2 The function $\bar{g}(t)$ for $a = 0$, compared with t^2 ($t \geq 0$) and $-2t^2$ ($t \leq 0$); $\rho(0) = -2$.

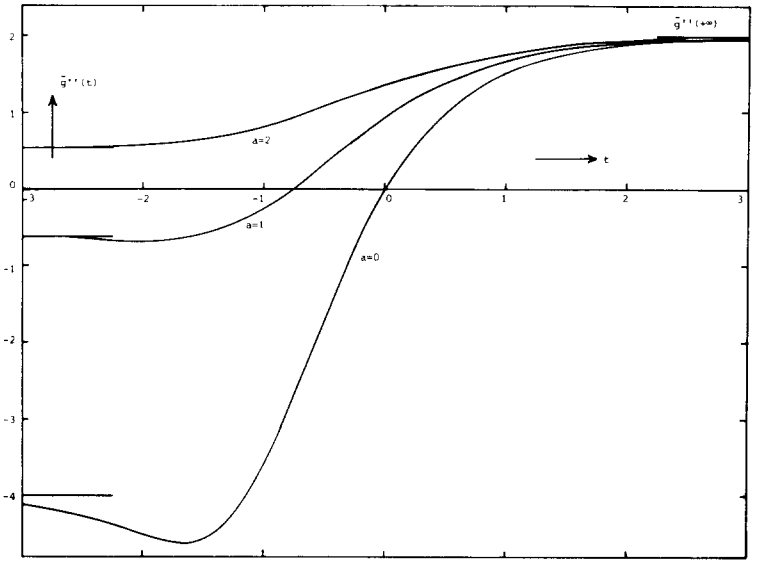

Figure 5.3 The function $\overline{g}''(t)$ for $a = 0$, 1 and 2. At right end $\overline{g}''(\infty) = 2$. Limits at left end are the values $\overline{g}'(-\infty)$.

5.2 *Approximations to the function ρ*

The asymptotic behaviour of $\rho(a)$ for large values of a has been derived by Dijkstra [4A] and there holds

$$\rho(a) = \rho_{as}(a) + O(\alpha^4) \quad , \quad \alpha = \frac{\pi}{2a\sqrt{a}} \quad , \quad a \to \infty,$$

where

$$\rho_{as}(a) = \frac{1 - \alpha + \frac{1}{2}\alpha^2 - \left(\frac{1}{6} + \frac{35}{8\pi^2}\right)\alpha^3}{1 + \alpha + \frac{1}{2}\alpha^2 + \left(\frac{1}{6} + \frac{35}{8\pi^2}\right)\alpha^3} .$$

The quality of this approximation may be deduced from Fig. 5.1 and Table 5.1 and it produces good results beyond $a = 2$. However for most applications of the theory, the parameter a lies in the range [0,1] and an expansion in Chebychev polynomials over this range has been constructed by Dijkstra [4A] with a method from [6]. The approximation reads

$$\rho_0(a) = \sum_{n=0}^{8} c_n T_n(x) \quad , \quad x = 2a - 1 \quad , \quad 0 \leqslant a \leqslant 1, \tag{5.1}$$

where

$$T_0(x) = 1 \quad , \quad T_1(x) = x \quad , \quad T_{n+1}(x) = 2xT_n(x) - T_{n-1}(x) \quad , \quad n = 1, 2, \ldots,$$

and the coefficients c_n are

n	c_n
0	− 1.029290352
1	+ 0.829400853
2	− 0.123888216
3	+ 0.015519846
4	− 0.001712787
5	+ 0.000170848
6	− 0.000015652
7	+ 0.000001332
8	− 0.000000106

The coefficient c_9 was found to be 8×10^{-9} which is in agreement with the error

$$| \rho(a) - \rho_0(a) | \leqslant 10^{-8} \quad , \quad 0 \leqslant a \leqslant 1.$$

Hence, the data in Table 5.1 for $\rho(a)$ with $0 \leqslant a \leqslant 1$ will be recovered to full accuracy if (5.1) is used and it will be clear that the computing time needed by (5.1) is vanishingly small when compared with the time required by (4.12).

5.3 Special cases

In this section some special values of a will be considered.

Case (i) $a = 0$

If the parameter s appearing in the rotating-disk equations (2.1) is set equal to 0, then a defined by (4.11) vanishes and the solution $\overline{g}$ of the problem (4.12) can be written as a confluent hypergeometric function (see [1]):

$$\overline{g}(t) = 3^{2/3} U\left(-\frac{2}{3}, \frac{3}{3}, \frac{t^3}{3} \right) \quad , \quad \rho(0) = -2. \tag{5.2}$$

In terms of the original variables the leading-order approximation to the tangential velocity $g(x)$ in the viscous interlayer becomes

$$g(x) \sim \pm \mu_1 A^{1/3} 3^{2/3} U\left(-\frac{2}{3}, \frac{2}{3}, \frac{Ax^3}{3} \right) . \tag{5.3}$$

At the origin $x = 0$ (point P_0, Fig. 4.1) this results yields

$$\begin{aligned} g(0) &\sim \pm \mu_1 A^{1/3} 3^{2/3} \Gamma(1/3)/\Gamma(-1/3), \\ g'(0) &\sim \mp \mu_1 A^{2/3} 3^{4/3} \Gamma(2/3)/\Gamma(-2/3). \end{aligned} \tag{5.4}$$

The quantity $|\rho(a)|$ has a global maximum over the range $0 \leqslant a \leqslant \infty$ attained at the boundary $a = 0$ with value 2. From the leading-order match theorem (4.13) it then follows that the ratio λ_1/λ_2 of amplitudes of two adjacent large hills is at most equal to $\rho^2 = 4$, while the ratio μ_2/μ_1 of the cell ranges is at most 2. For an application of these results see Sec. 7.

Case (ii) $a = 0.44274662$.

In this case we have $\rho(a) = -1$, so that (4.13) yields

$$\lambda_2 = \lambda_1 \quad , \quad \mu_2 = \mu_1 \quad \text{if} \quad s^2 = 0.44274662(\lambda_1 \mu_1^2)^{4/3}.$$

Hence – to leading order – the two adjacent large hills will be identical, the only difference being a change of sign in g. Of course, the argument may be repeated and a chain of large hills can be constructed (all with the same value of λ and μ) where the ultimate behaviour, i.e. grow or decay, then clearly depends on higher-order terms. For further elucidation of the importance of this special value of ρ we refer to [9].

Case (iii) $a = 1.42111689$

For this value of a the function $\rho(a)$ vanishes. Hence, under the condition

$$s^2 = 1.42111689(\lambda_1 \mu_1^2)^{4/3}$$

the continuation of an inviscid large hill through a viscous layer in negative x direction will be the parabola (4.10) proceeding without bound as $x \to -\infty$, while g becomes exponentially small. Clearly this situation is very sensitive to the effect of higher-order terms in the perturbation expansion. The decay of $\bar{g}$ and $\bar{g}''$ in the viscous layer has been depicted in Fig. 5.4.

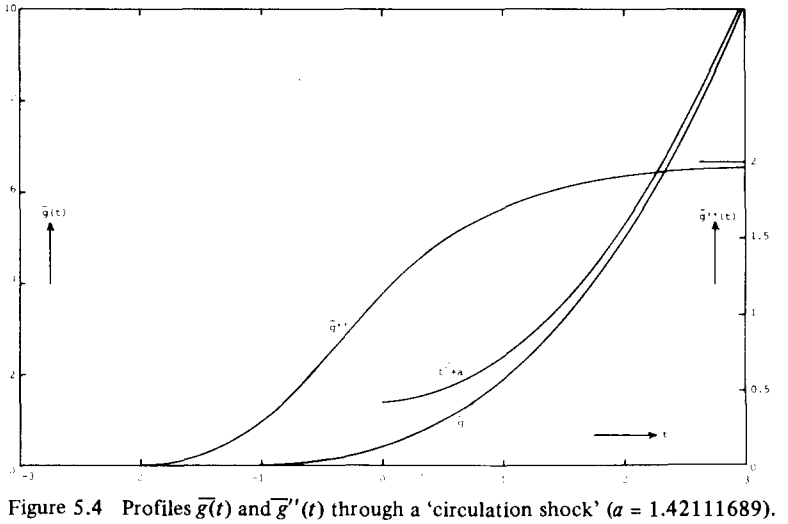

Figure 5.4 Profiles $\bar{g}(t)$ and $\bar{g}''(t)$ through a 'circulation shock' ($a = 1.42111689$).

If second-order effects are neglected we might interpret this special case as a 'circulation shock': at one side of the viscous interlayer there is a certain rotation ($g \neq 0$) whereas at the other side there is no rotation at all and the velocity vector has only axial and radial components. For further details, see [9].

6. Second-order results for $s = 0$

The theory presented above can be extended to higher order; indeed, Dijkstra [4A] has developed a complete second-order theory for the special case $s = 0$ and it is believed that second-order results can be obtained in the same way for general values of the parameter s. The results of the second-order theory ($s = 0$) will now be presented.

In the limit (4.1) we have for two adjacent large hills (Fig. 4.1) according to the leading-order match theorem with $s = 0$:

$$\lambda_2\mu_2^2 = \lambda_1\mu_1^2 \quad , \quad \rho(0) = -2 \Rightarrow \lambda_1/\lambda_2 = 4 \quad , \quad \mu_2/\mu_1 = 2. \tag{6.1}$$

The present author [4A] has shown that these relations are perturbed by an amount $O(\mu^2)$ when second-order effects are included, e.g.

$$\frac{\lambda_2\mu_2^2}{\lambda_1\mu_1^2} = 1 + 24.283166\, R_1^{2/3} \quad , \quad R_1 = \mu_1/\lambda_1 = O(\mu_1^3) \to 0 \tag{6.2}$$

where the correction of order μ_1^2 represents the effect on f of the nonsymmetric shape of g in the viscous interlayer. In addition this effect produces the following approximation to the value of f at P_0 (Fig. 4.1):

$$f(P_0) \sim -Qg^2(P_0)/A \quad , \quad A = \lambda_1\mu_1^2 \tag{6.3}$$

with $g(P_0)$ given by (5.4) and coefficient Q equal to

$$\begin{aligned} Q &= \int_0^\infty t^2 \exp(-\tfrac{1}{3}t^3)\tilde{g}^2(t)dt = 2.060749186, \\ \tilde{g}(t) &= U\left(-\frac{2}{3}, \frac{2}{3}, \frac{t^3}{3}\right) \Gamma(-1/3)/\Gamma(1/3). \end{aligned} \tag{6.4}$$

The constant Q is of fundamental importance in the theory of large hills since it also appears in the papers by Ockendon [7] and Bodonyi [2]. The reason for this is that the ratio (at P_0) of the terms ff'' and g^2 in eq. 2.1 must have a particular value in the limit considered, otherwise the solution when continued from P_0 in positive x-direction explodes exponentially. In fact, it follows from (6.3) that at P_0 (in the limit (4.1))

$$-\frac{ff''}{2g^2} = Q, \tag{6.5}$$

where (4.7) has been used to replace $2\lambda_1\mu_1^2$ by f''. Another quantity, relating values at P_0 and P_1 (Fig. 4.1), is

$$\frac{f(P_0)}{f(P_1)} * \frac{g^2(P_1)}{g^2(P_0)} = -Q(1 - 5.384733524\, R_1^{2/3}), \quad R_1 = \mu_1/\lambda_1, \tag{6.6}$$

in which again the constant Q (6.4) appears. Note that the left-hand side in (6.6) is independent of the scales in f and g.

The distance P_0P_1 (Fig. 4.1), which is $\pi/(2\mu_1)$ in first-order theory, involves logarithmic terms of the perturbation parameter when higher-order effects are incorporated. In fact there holds

$$\mu_1 * P_0P_1 = \frac{\pi}{2} + \frac{8}{9} R_1 \ln R_1 + 0.18737422\, R_1 \quad , \quad R_1 = \mu_1/\lambda_1. \tag{6.7}$$

This formula expresses the fact that the quantities Δ_1 and Δ_2 in eq. (4.2) are different from zero when second-order effects are considered.

We conclude this section by stating some results relating quantities at infinity with large-hill parameters. The possibility of matching a large hill with the exponential decay at infinity was put forward by Ockendon [7], see case I at the end of Section 3. The work necessary to establish the required relationship was performed by Kuiken [5] for the case $s = 0$. His asymptotic result for $f(\infty)$ has been compared with accurate numerical results and there appeared to be a systematic disagreement between theory and numerical solution. To resolve this problem we re-did the Kuiken calculation and obtained a leading-order coefficient significantly different from his value. After correction the result became:

$$f(\infty) = (\lambda\mu^2)^{1/3}\,(-1.209707087 + 1.573089\, R^{2/3}) \tag{6.8}$$

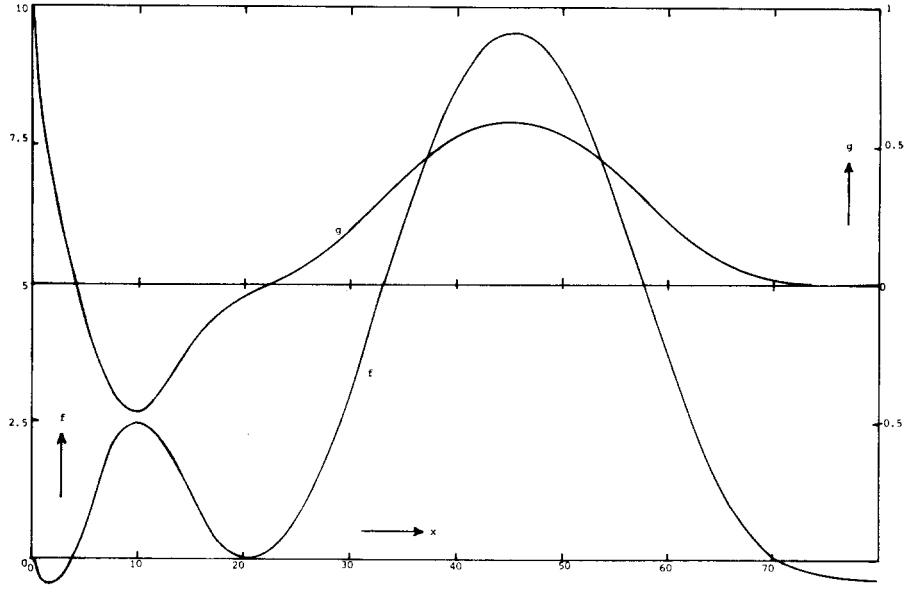

Figure 6.1 The solutions $f(x)$ and $g(x)$ at $s = 0$ for the third solution branch of the rotating-disk problem.

where $R = \mu/\lambda$ and λ and μ are the parameters of the first large hill (counted from infinity in the direction of the disk) appearing in the solution. In addition to (6.8) the following new result for g has been obtained

$$\lim_{x\to\infty} \frac{g(x)}{f'(x)} = \mp\, 0.5122093866\, R^{1/3}, \tag{6.9}$$

where the upper sign will produce positive values of g in the first large hill.

All the results listed in this section refer to the case $s = 0$ and their quality will be investigated in the next section where a comparison with numerical results will be made.

7. Comparison of theoretical with numerical results

The asymptotic results presented in this paper will now be compared with accurate numerical results calculated by Zandbergen [9]. In Section 7.1 the leading-order match theorem (4.13) will be verified for some cases with $s \neq 0$ and in Section 7.2 the second-order results for $s = 0$ will be considered.

7.1 The case $s \neq 0$

By continuing rotating-disk solutions for $s = 1 + \epsilon$ through the disk Zandbergen [9] has calculated numerical solutions to the equations (2.1) in which sequences of large hills appear. From these solutions we have selected two cases for the present comparison. Remote boundary

TABLE 7.1

Numerical and theoretical results for two adjacent hills in the configuration of Fig. 4.1 with ρ near to -1 and $\mu \sim 0.04$.

Quantity	Num. solution (source [9])	Asymptotic value (present theory)	Eq.	Abs. Error
$f(P_1)$	1024.4	$\lambda_1 = 1023.9$	(2.12)	definition
$g(P_1)$	−43.661	$\mu_1 = 0.042621$	(2.12)	definition
$f''(P_1)$	−3.7198	$-2\lambda_1\mu_1^2 = -3.7200$	(3.6)	0.0002
P_0P_1	36.847	$\pi/(2\mu_1) = 36.855$	(2.11)	0.008
$f(P_0)$	0.53109	$s^2/A_1 = 0.53763$	(4.10)	0.007
$f''(P_0)$	3.7361	$2\lambda_1\mu_1^2 = 3.7200$	(4.10)	0.02
$f(P_2)$	995.74	$\lambda_2 = 995.21$	(2.12)	definition
$g(P_2)$	43.294	$\mu_2 = 0.043479$	(2.12)	definition
λ_1/λ_2	1.0288	$\rho^2 = 1.0189$	(4.13)	0.01
μ_2/μ_1	1.0201	$\lvert\rho\rvert = 1.0094$	(4.13)	0.01

$s = 1$; $A_1 = \lambda_1\mu_1^2 = 1.8600$; $a = s^2/A_1^{4/3} = 0.43717$;
$\rho(a) = -1.0094$ (eq. 5.1)

TABLE 7.2

Numerical and theoretical results for two adjacent hills in the configuration of Fig. 4.1 with ρ near to -0.8 and $\mu \sim 0.003$.

Quantity	Num. solution (source [9])	Asymptotic value (present theory)	Eq.	Abs. Error
$f(P_1)$	130874.3	$\lambda_1 = 130873.6$	(2.12)	definition
$g(P_1)$	445.2868	$\mu_1 = 0.003402401$	(2.12)	definition
$f''(P_1)$	-3.030073	$-2\lambda_1\mu_1^2 = -3.030072$	(3.6)	0.000001
P_0P_1	461.6728	$\pi/(2\mu_1) = 461.6729$	(2.11)	0.0001
$f(P_0)$	0.6600119	$s^2/A_2 = 0.6600143$	(4.10)	0.000002
$f''(P_0)$	3.030169	$2\lambda_2\mu_2^2 = 3.030280$	(4.10)	0.0001
$f(P_2)$	207021.4	$\lambda_2 = 207020.7$	(2.12)	definition
$g(P_2)$	-560.0601	$\mu_2 = 0.002705325$	(2.12)	definition
λ_1/λ_2	0.6321764	$\rho^2 = 0.6322325$	(4.13)	0.00006
μ_2/μ_1	0.7951223	$\lvert\rho\rvert = 0.7951305$	(4.13)	0.00001

$s = 1.000007$; $A_2 = \lambda_2\mu_2^2 = 1.515140$; $a = s^2/A_2^{4/3} = 0.5746487$;
$\rho(a) = -0.7951305$ (eq. 5.1)

conditions will be ignored in this section since we will focus our attention on the interrelation between two adjacent large hills in the configuration of Fig. 4.1. For the two cases considered the orders of magnitude of the parameters μ differ by a factor > 10 so that the errors in the leading order theory (which are $O(\mu^2)$) differ by a factor > 100. The actual comparison is made by arranging several relevant quantities in tabular form (Tables 7.1 and 7.2) and it is clear that a large reduction of the error appears as the level of the parameter μ is reduced: the errors are smaller if the hills are closer to the limit (4.1). This demonstrates the asymptotic nature of the present theory. On the other hand it will be clear that the theory provides a powerful means to penetrate analytically in regions where large hills (or sequences of large hills) are present. In fact the present theory can be used to avoid any numerical calculation for those regions in which μ is small enough

7.2 The case $s = 0$

Zandbergen [9] has revealed the complete structure of multiple solutions to the rotating-disk problem (2.1) and it is now clear that e.g. for $s = 0$ there are infinitely many solutions to the Von Karman problem, each of which satisfies the boundary conditions at the disk and at infinity. It will be convenient to count the solutions from $n = 1$ onwards and to let $n = 1$ correspond with the classical Von Karman boundary-layer solution. Then the solution $f_n(x)$ consists of $f_1(x)$ near the disk followed by $(n-1)$ hills and the height of the hills grows asymptotically with a factor 4 (see Fig. 6.1 for $f_3(x)$). Beyond the last hill the solution merges with the exponential decay at infinity, viz.

$$f_n(x) \sim f_n(\infty) + \text{exp. small terms}, \quad x \to \infty.$$

The numbers $f_n(\infty)$ appear to have an accumulation point, indicated by $f_\infty(\infty)$, which corresponds to the limit-solution branch of the problem. An accurate value for $f_\infty(\infty)$ can be obtained by applying a well-defined extrapolation technique to values for $f_n(\infty)$ with $1 \leqslant n \leqslant 7$. The numerical results for these values of n have been tabulated in Table 7.3, where λ_n and μ_n refer to the largest hill in the solution (f_n, g_n).

According to the theory we must have

$$\lambda_n/\lambda_{n-1} = 4 + O(\mu_n^2) \quad , \quad \mu_{n-1}/\mu_n = 2 + O(\mu_n^2).$$

where the error term with subscript n will be 4 times as small as at the level $(n-1)$. Hence, we can apply Richardson extrapolation in precisely the same way as in the Romberg algorithm for the trapezoidal rule. The extrapolation for the ratio of the quantities λ has been performed in Table 7.4 and it is clear that the extrapolation is correct.

The same procedure can be applied to the ratio of μ_n with a similar result. It follows that the quantities $\lambda_n\mu_n^2$ can be extrapolated in the same way and one obtains

$$\lim_{n\to\infty} \lambda_n\mu_n^2 = (\lambda\mu^2)_\infty = 0.02860302601.$$

In the same limit (6.8) becomes

$$f_\infty(\infty) = -1.209707087\,(\lambda\mu^2)_\infty^{1/3} = -0.3699566901.$$

TABLE 7.3

Quantities relevant to the first 7 solutions of the Von Karman problems (s = 0)

n	$-f_n(\infty)$	λ_n	$1000\mu_n$
1	0.8844741102	--	--
2	0.4477233339	2.497764172	186.7367737
3	0.3873746413	9.572567631	62.48933600
4	0.3741975175	37.78586389	28.43748256
5	0.3710099805	150.6370591	13.89364721
6	0.3702195833	602.0419285	6.906944470
7	0.3700223866	2407.661458	3.448510653

TABLE 7.4

Richardson extrapolation for ratio of λ_n

n	λ_n/λ_{n-1}	$O(\mu^2) \to 0$	$O(\mu^4) \to 0$
3	3.832454536		
4	3.947307070	3.985591248	
5	3.986598256	3.999695318	4.000635589
6	3.996638889	3.999985767	4.000005130
7	3.999159102	3.999999173	4.000000067

On the other hand the data $f_n(\infty)$ may be extrapolated to the limit and one finds after removing terms of $O(\mu^2)$ and $O(\mu^4)$:

$$f_\infty(\infty) = -0.3699566902.$$

From the mutual agreement between theoretical and numerical results it can be inferred that
(i) The accuracy of the numerical results is beyond all doubt
(ii) The theory can take over when the numerical method becomes too laborious.

To illustrate these conclusions we finally present an explicit formula for $f_n(\infty)$:

$$-f_n(\infty) = 0.3699566901 + 1.076226*4^{-n} + 2.3956*4^{-2n} + 4.5*4^{-3n}.$$

At $n = 1$, where the solution $f_1(x)$ does not contain any hill at all, this formula produces

$$-f_1(\infty) \sim 0.859 \quad \text{(error 0.025)}$$

while at $n = 3$ the error is already at the level 10^{-7}.

8. Concluding remarks

The theory presented in this paper is a powerful means to obtain insight into the behaviour of sequences of large hills or into possible solution-structures of the governing equations. It also demonstrates the power of the method of matched asymptotic expansions. Furthermore it furnishes an independent check on results obtained with some numerical method of solution. It is believed that the present theory can be applied also to the two-disk problem for large Reynolds numbers. It is planned to use the present results for the construction of the limit-solution branch for the single rotating-disk problem.

Acknowledgement

Several stimulating and helpful discussions with P. J. Zandbergen are gratefully acknowledged.

Appendix A

Theorem. Let $f \in C^4(-\infty,\infty)$ be a solution to the differential equation

$$f''' - ff'' + \tfrac{1}{2}f'^2 = -2s^2 \quad , \quad ' = d/dx \quad , \quad -\infty < x < \infty, \tag{A.1}$$

such that for constants A, B and C:

$$f(x) = Ax^2 + Bx - C + o(1) \quad , \quad x \to \infty \quad , \quad A > 0. \tag{A.2}$$

Then

$$f(x) \equiv Ax^2 + Bx + C, \qquad -\infty < x < \infty, \tag{A.3}$$

$$B^2 - 4AC = -4s^2, \tag{A.4}$$

$$f(x) \equiv A\left(x + \frac{B}{2A} \right)^2 + s^2/A. \tag{A.5}$$

Proof. We differentiate the differential equaiton (A.1) and multiply the result by $\exp(-F)$ where

$$F(x) = \int_0^x f(t)dt \sim Ax^3/3 \quad , \quad x \to \infty. \tag{A.6}$$

It follows that

$$[\exp(-F)f'']' = 0,$$

hence

$$f''(x) = D \exp(F(x)).$$

From (A.6) we infer that in case $D \neq 0$ the function f'' (and hence f) explodes exponentially for $x \to \infty$ since $A > 0$. This contradicts (A.2). Therefore, $D = 0$ so that $f''' \equiv 0$ and f must be a parabola, which in view of (A.2) must be (A.3). Substituting the solution (A.3) into (A.1) we obtain (A.4). Combination of (A.3) and (A.4) yields the result (A.5).

REFERENCES

[1] Abramowitz, M. and Stegun, I. A., *Handbook of mathematical functions*. Nat. Bur. Standards, Washington, 1966.

[2] Bodonyi, R. J., On rotationally symmetric flow above an infinite rotation disk, *J. Fluid Mech.* 67 (1975) 657-666.

[3] Bulirsch, R. and Stoer, S., Numerical treatment of ordinary differential equations by extrapolation methods, *Num. Math.* 8 (1966) 1-13, 93-104.

[4] Dijkstra, D. and Zandbergen, P. J., Some further investigations on non-unique solutions of the Navier-Stokes equations for the Karman swirling flow, *Archives of Mechanics* 30 (1978) 411-419 (Warszwawa).

[4A] Dijkstra, D., On the relation between adjacent inviscid cell type solutions to the rotating disk equations, *Memorandum THT*, Department TW (1979).

[5] Kuiken, H. K., The effect of normal blowing on the flow near a rotating disk of infinite extent, *J. Fluid Mech.* 47 (1971) 789-798.

[6] *Modern Computing Methods*, N.P.L. notes on applied science 16; H.M. Stationery Office London (1961).

[7] Ockendon, H., An asymptotic solution for steady flow above an infinite rotating disk with suction, *Quart. J. Mech. Appl. Math.* 25 (1972) 291-301.

[8] Zandbergen, P. J. and Dijkstra, D., Non-unique solutions of the Navier-Stokes equations for the Karman swirling flow, *J. Engg. Math.* 11 (1977) 167-188.

[9] Zandbergen, P. J., New solutions of the Karman problem for rotating flows, *Proc. IUTAM symposium on approximation methods for Navier-Stokes Problems*, Paderborn, West-Germany (september 1979).